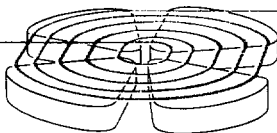


GANIL



*Invited talk to the International
Workshop on "nuclear dynamics at medium
and high energies"
Bad Honnef (FRG), October 10-14, 1988*

EXPLOSIONS IN LANDAU VLASOV DYNAMICS

E. SURAUD
Kernfysisch Versneller Instituut, Zernikelaan 25,
AA GRONINGEN, The Netherlands

D. CUSSOL, Ch. GREGOIRE
GANIL, BP 5027, F 14021 CAEN CEDEX, France

D. BOILLEY, M. PI, P. SCHUCK
Institut des Sciences Nucléaires, 53 Av. des
Martyrs, F 38026 GRENOBLE CEDEX, France

B. REMAUD, F. SEBILLE
Université de Nantes, F 44072 NANTES CEDEX, France

GANIL P 88 16
(KVI 771).

EXPLOSIONS IN LANDAU VLASOV DYNAMICS

E. SURAUD¹⁾

Kernfysisch Versneller Instituut, Zernikelaan 25, 9747 AA Groningen,
The Netherlands

D. CUSSOL, Ch. GRÉGOIRE²⁾

GANIL, B.P. 5027, F 14021 Caen Cedex, France

D. BOILLEY, M. PI³⁾, P. SCHUCK

Institut des Sciences Nucléaires, 53 Av. des Martyrs, F 38026 Grenoble
Cedex, France

B. REMAUD, F. SÉBILLE

Université de Nantes, F 44072 Nantes Cedex, France

ABSTRACT

A microscopic study of the quasi-fusion/explosion transition is presented in the framework of Landau-Vlasov simulations of intermediate energy heavy-ion collisions (bombarding energies between 10 and 100 MeV/A). A detailed analysis in terms of the Equation of State of the system is performed. In agreement with schematic models we find that the composite nuclear system formed in the collision does explode when it stays long enough in the mechanically unstable region (spinodal region). Quantitative estimates of the explosion threshold are given for central symmetric reactions (Ca+Ca and Ar+Ti). The effect of the nuclear matter compressibility modulus is discussed.

1) Present address : GANIL, Caen, France

2) Present address : SUNY, Stony-Brook, USA

3) Present address : Universitat Barcelona, Spain

1. INTRODUCTION

One of the most exciting features of intermediate energy heavy ion reactions ($E/A \sim 10-100$ MeV and typical compressions less than twice the saturation density) is the transition from quasi fusion like reactions ($E/A \lesssim 20$ MeV) to explosion/fragmentation processes. Beyond its intrinsic interest for heavy ion physics it probably should give us unique fingerprints of the nuclear Equation of State (EOS) at high excitation energies. Moreover this "transition" - which has often been related to thermodynamical well established phase transitions [1] - occurs in a finite system where dynamical effects are presumably dominant, thus providing interesting insights in the statistical physics of non macroscopic systems far from equilibrium [2]. While the possible scenario for such a dynamical break up of the nucleus can be roughly figured out from schematic models [3,4] only microscopic dynamical models can allow for a semi-quantitative description of this phenomenon [5,6]. Moreover such calculations are of prime importance for a proper definition of the initial state of the statistical calculations which describe the final products of fragmentation in static pictures [7,8,9].

In this work we investigate this fusion/explosion transition using a numerical simulation of the Landau-Vlasov equation (LVE) [5]. We show, in agreement with qualitative models [5,10] that the explosion occurs when the excited nuclear composite system actually enters the region of mechanical instability and stays long enough (≥ 120 fm/c) in this forbidden region. Due to our microscopic approach we consistently take into account finite size and dynamical effects such as the energetic emission of pre-equilibrium particles which strongly influences the energy balance of the reaction.

2. THE LANDAU-VLASOV EQUATION

The Landau-Vlasov equation is a kinetic equation for the one-body distribution function (Wigner function) $f(\vec{r}, \vec{p}, t)$ and can be written as

$$\frac{\partial f}{\partial t} + \frac{\vec{p}}{m} \cdot \vec{\nabla}_{\vec{r}} f - \vec{\nabla}_{\vec{p}} U(\vec{r}) \cdot \vec{\nabla}_{\vec{p}} f = I_{\text{coll}}[f] \quad (1)$$

in the case of a local mean-field potential $U(\vec{r})$. In our calculations we use schematic oversimplified Skyrme interactions whose t_0, t_3 parameters have been fit to reproduce nuclear matter saturation ($\rho_0 \approx 0.15 \text{ fm}^{-3}$, $E/A \approx -16$ MeV and $K_\infty \approx 200$ MeV). In eq. (1) I_{coll} stands for the collision integral which is expressed in the Uehling-Uhlenbeck approximation [11], namely

$$I_{\text{coll}}[f] = \frac{g}{4m^2} \frac{1}{\pi^3 \hbar^3} \int d\vec{p}_2 d\vec{p}_3 d\vec{p}_4 \frac{d\sigma}{d\Omega} \times \delta(\vec{p} + \vec{p}_2 - \vec{p}_3 - \vec{p}_4) \delta(p^2 + p_2^2 - p_3^2 - p_4^2) \\ \left\{ (1-\bar{f})(1-\bar{f}_2)f_3f_4 - (1-\bar{f}_3)(1-\bar{f}_4)f_2f \right\} \quad (2)$$

where the \bar{f} represent occupation numbers and g is the degeneracy (2 for spin saturated systems). Equation (1) together with the collision integral eq. (2) has been extensively studied in the past few years by various groups and we refer the reader to their published results for more details [5,6,12].

We would however like to point out the fact that merely simulations rather than solutions of the Landau-Vlasov equation are presently available. Practically all these simulations are based on (pseudo) particle methods [13], that is the Wigner distribution f is projected on a swarm of elementary functions (delta functions or gaussians) whose centroids evolve in phase space according to classical Hamilton equations of motion under the force field generated by the one body mean-field potential. In the so-called VUU approach each particle represents one nucleon [6] while in the LVE calculations the Wigner distribution f is projected on a larger basis of typically some thousands of pseudo-particles [5]. To correct for the poor statistical representation of the phase space in the VUU approach, parallel runs have to be taken into account. In both cases (LVE/VUU) the collision integral eq. (2) is then simulated by 2-body collisions between pseudo particles. Two pseudo particles encounter a collision if during a time step Δt they reach their distance of closest approach d_{min} and if d_{min} is smaller than a cutoff radius $R_0 = \sqrt{\tilde{\sigma}/\pi}$ given by the angle averaged nucleon-nucleon cross section σ . Although this prescription sounds reasonable enough it should be realized how σ enters the process in a now trivial way, thus giving rise to an effective cross section $\tilde{\sigma}$. Indeed, contrarily to the case of Boltzmann-like equations, if one artificially increases σ towards infinity $\tilde{\sigma}$ tends towards a finite limit, completely different from the expected hydrodynamical limit. This "surprising" asymptotic behaviour actually proves the now trivial mapping between simulations and conventional equations.

It is hence interesting to try to figure out how close are LVE or VUU simulations [5,6] to the solution of eq. (1). Work is in progress in that direction [14] using an analytical solution of the Boltzmann equation [15]. On a practical level a crucial check of the simulations is the fact that they are independent of the numerical parameters namely the time step and, in the case of LVE the number of pseudo particles. This can be explicitly checked in both cases for the quantities of interest in the actual calculations.

3. THE SPINODAL PUZZLE

As already mentioned in the introduction, due to the short time scales involved, composite systems formed during heavy-ion collisions presumably explode via dynamical instabilities and a scenario of the transition can be roughly figured out from schematic models [3,4]. In these models it was shown that, if one assumes that the expansion of the initially compressed system is isentropic, the actual explosion occurs when the system crosses the isentropic spinodal line, namely enters a region of mechanical instability. More precisely as was recently investigated by Pethick and Ravenhall [10] entering the spinodal region is a necessary but not sufficient condition for the excited nucleus to explode. Indeed the spinodal region is a region of the EOS in which even small fluctuations are able to disrupt the system; that is, provided the nucleus stays long enough in the unstable region any small density fluctuation may grow up to be comparable in size to the actual nuclear density hence breaking the system into pieces. In this picture 2 quantities govern the whole phenomenon, the growth rate Γ , directly connected to the sound velocity and the transit time in the spinodal region Δt_s . The explosive cocktail thence simply stems from the integral

$$\int_{\Delta t_s} \Gamma dt \quad (3)$$

A schematic picture of the EOS and the corresponding unstable regions is presented in figure 1 for the sake of completeness.

A quantitative description of the fusion/explosion threshold however requires microscopic simulations of the nucleus-nucleus collisions, in order to introduce in a proper way finite size effects (surface, Coulomb) and a reasonable dissipative dynamics. The pre-equilibrium particles, in particular, are to be taken into account, as they can carry out a large amount of the available energy and should hence not be counted in the energy balance leading to the actual explosion. In order to point out this overall complexity we show in figure 2 the time evolution of the various energy components entering a typical reaction in the energy range of interest. In the particular case of figure 2 the reaction leads to a fusion of the Ar and Au nuclei and it is interesting to note how much of the total available energy (~ 8 MeV/A) is really of thermal nature (~ 2 MeV/A), while 3 MeV/A are taken away by the pre-equilibrium particles and 2 MeV/A are of compressional origin, 1 MeV/A being pure kinetic collective energy (see section 4 for more precise definitions of these quantities). This energy balance has hence to be taken

into account properly for estimating for example the final temperature of the hot residue (in the case of figure 2 the temperature is thus of order 4 MeV).

Schematic Equation of State

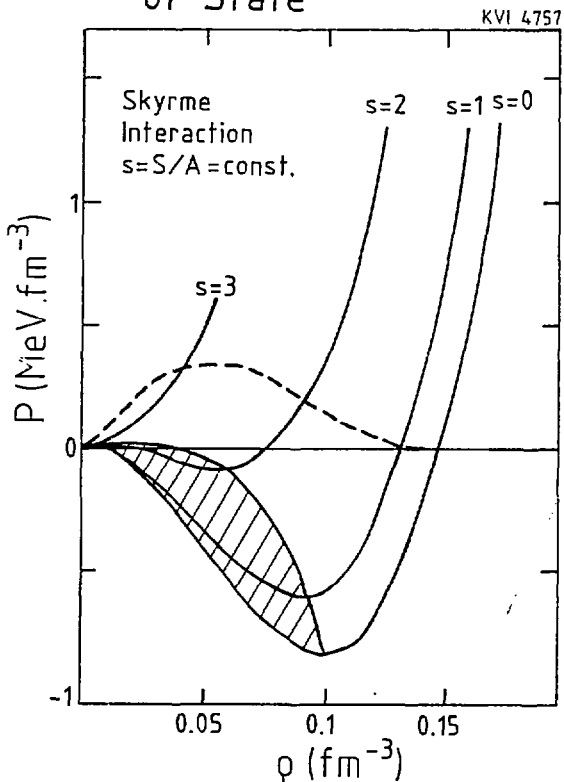


FIGURE 1

Schematic representation of a typical Equation of State $P(\rho)$ (pressure P in $\text{MeV} \text{ fm}^{-3}$ versus density ρ in fm^{-3}) obtained with Skyrme forces. We have indicated 4 isentropic lines ($S/A = 0, 1, 2$ and 3 in Boltzmann constant unit) and the isentropic spinodal region (hatched area). Also is shown for completeness the liquid-gas coexistence line (dashed line).

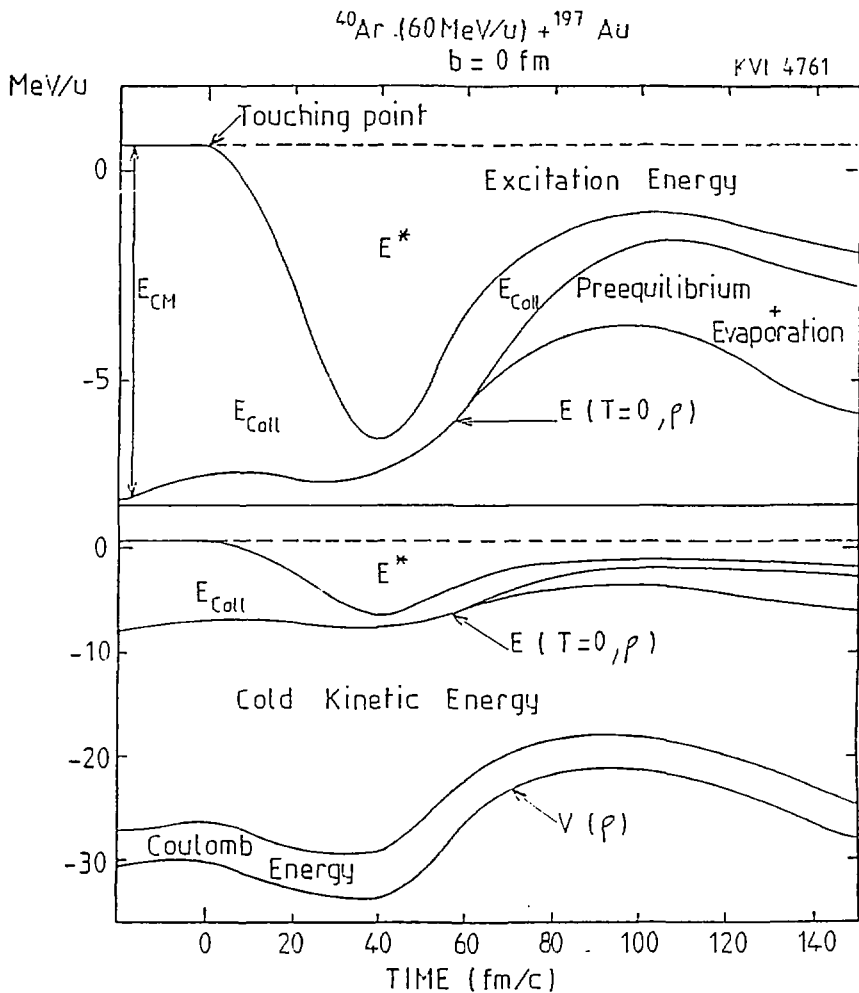


FIGURE 2

Energy transfers in an head on $^{40}\text{Ar}+^{197}\text{Au}$ collision at 60 MeV/A bombarding energy. The upper part shows the time evolution of the thermal excitation energy E^* (Eq. (8)) and of the kinetic collective energy E_{coll} (Eq. (4)). Also are mentioned the cold potential energy $E_{\text{int}}^0 = E(T=0, \rho)$ (see text) and the pre-equilibrium plus evaporation components. In the lower part are given all energy contributions with a reduced scale.

4. THE LVE ANALYSIS OF THE FUSION/EXPLOSION TRANSITION

While the microscopic simulation virtually includes most of the quantities of interest one nevertheless has to analyse the results of the calculations in terms of "macroscopic" quantities, in order to understand how an excited nuclear system may enter the spinodal region. For this purpose we first separate the total energy E_{tot} into 2 contributions:

- the kinetic collective energy

$$E_{coll} = \frac{1}{2} m \int \frac{\vec{j}^2}{\rho} d\vec{r} \quad (4)$$

where m is the nucleon mass, \vec{j} the current vector

$$\vec{j}(\vec{r}) = \int \vec{p}/m f(\vec{r}, \vec{p}, t) d\vec{p} \quad (5)$$

and ρ the local density

$$\rho(\vec{r}) = \int f(\vec{r}, \vec{p}, t) d\vec{p} \quad (6)$$

- the intrinsic (potential) energy

$$E_{int} = E_{tot} - E_{coll} \quad (7)$$

This intrinsic energy E_{int} may in turn be splitted into 2 components namely a compressional and a thermal one. The thermal excitation energy is thence defined as

$$E^* = E_{int} - E_{int}^0 \quad (8)$$

where the 0 index labels the "cold" limit of the intrinsic energy. More precisely E_{int}^0 is calculated as a function of the density of the system by letting a nucleus in its ground state expand and explode, within having switched off two body collisions for preventing heat production. In terms of the equation of state (see also fig. 4) $E_{int}(\rho)$ represents the actual trajectory of an excited system while E_{int}^0 corresponds to the zero temperature or zero entropy line. In order to interpret our results in terms of the EOS one has also to define an average density $\langle \rho \rangle$,

$$\langle \rho \rangle = \frac{1}{A} \int \rho^2(\vec{r}) d\vec{r} \quad (9)$$

We have also used alternative definitions for $\langle \rho \rangle$ (integration over a central \vec{r} -space cell, ...) without finding major differences in the results.

In figure 3 is plotted the time evolution of $\langle \rho \rangle$ (Eq. (9)) for the Ca+Ca central reaction at various laboratory energies between 20 and 100 MeV/A. While at low energies ($E/A < 40$ MeV) the compression/expansion sequence generates a long-living large amplitude monopole oscillation, one can already see that at higher energies the system is unable to recontract after the expansion and indeed explodes. More precisely by plotting the time evolution of E_{coll} and E_{int} one can check that beyond 40 MeV/A the collective energy remains much larger than the potential energy E_{int} at any time during the expansion. In other words the system had enough kinetic energy to cross the potential barrier. An even more interesting way of looking at the results is

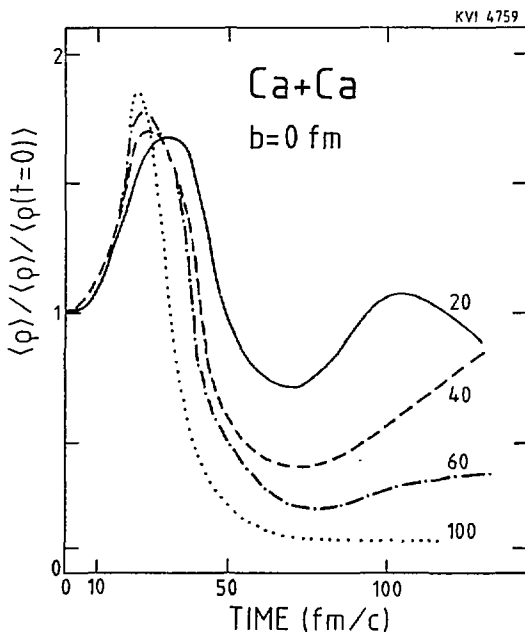


FIGURE 3

Time evolution of the average density $\langle \rho \rangle$ (Eq. (9), in fm^{-3}) for the $^{40}\text{Ca}+^{40}\text{Ca}$ reaction at various bombarding energies. Note the almost saturating maximum compression.

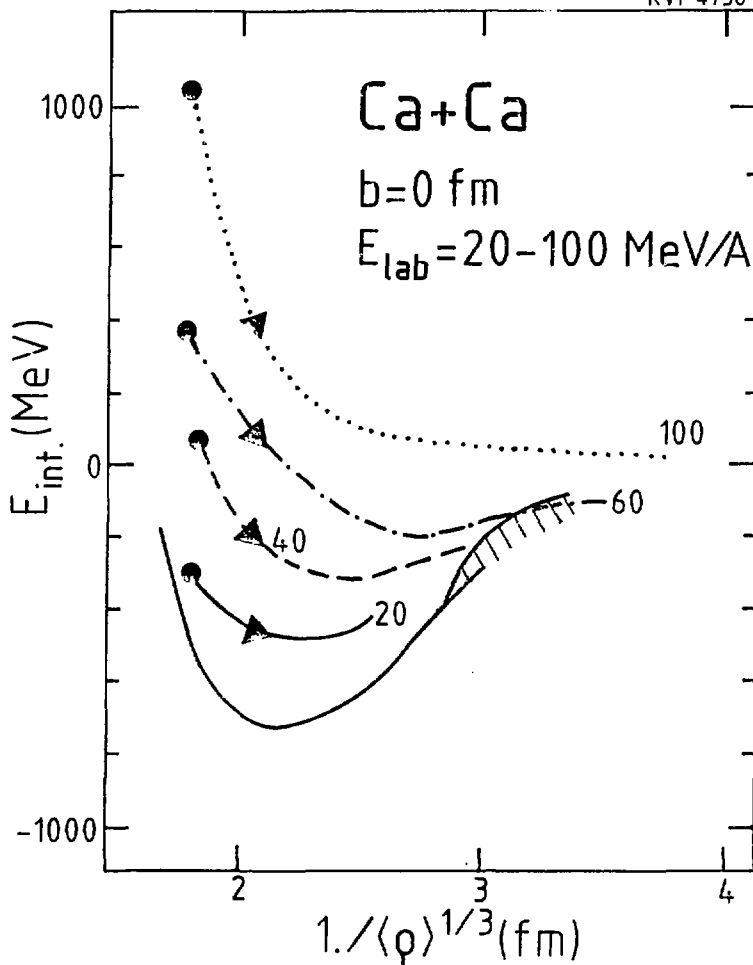


FIGURE 4

"Equation of State" of the $^{40}\text{Ca} + ^{40}\text{Ca}$ reaction between $E_{\text{lab}} = 20$ and 100 MeV/A . E_{int} (Eq. (7), in MeV) is plotted versus $1/\langle \rho \rangle^{1/3}$ (see Eq. (9), in fm). Also is indicated a rough evaluation of the spinodal region (hatched area) corresponding to this EOS (see text).

to plot E_{int} as a function of $\langle\rho\rangle$ in order to define an Equation of State for the reaction. It should be noted that, as one can check that the entropy of the expanding system is almost constant as a function of time, E_{int} hence exactly represents the relevant thermodynamical potential in this situation (contrarily to an isothermal expansion which would require the free energy!). The "EOS" of the Ca+Ca reaction is plotted in figure 4 where E_{int} is shown as a function of $1/\langle\rho\rangle^{1/3}$ which represents the size of the system. At low energy ($E_{lab} < 20-40$ MeV/A) the monopole oscillation of figure 3 here corresponds to explore the vicinity of the "equilibrium" state, namely the point of lowest energy, just as for a standard "cold" small amplitude monopole mode. At 60 MeV/A laboratory energy the system does explode but a potential barrier is still present, contrarily to the case at 100 MeV/A for which the intrinsic energy is monotonically decreasing. Calculating the spinodal line for this EOS (figure 4) is numerically difficult as it involves second derivatives (local compressibility $K(\langle\rho\rangle)$). We have hence assumed that the spinodal density ($K=0$) can be roughly taken as 60% of the "equilibrium" density [16]. When plotting this approximate line one finds that it is crossed just above 40 MeV/A lab energy in agreement with our previous conclusion.

5. MORE ABOUT THE INSTABILITY

In order to go a step further in our analysis of the onset of the mechanical instability we are going to try to evaluate the transit time in the spinodal region as suggested by recent model calculations [10]. In their way to characterize the spinodal instability the authors of Ref. [10] show that the first unstable multipole mode is the quadrupole one but the monopole mode merges quite close to the quadrupole, higher multipolarities appearing only when one experiences deeper insights in the spinodal region. This essentially means that if quadrupole modes are presumably the easiest ones to excite at low energy, as soon as energy increases monopole like instabilities may become of prime importance. In order to estimate the approximate multipolarity of the collective velocity field associated to the expansion we have made a comparison between E_{coll}^{monop} (Eq. 4) and the "monopole-like" collective energy

$$E_{coll}^{monop} = \frac{1}{2} m \int \frac{(\vec{j} \cdot \vec{r})^2}{\rho \cdot \vec{r}^2} d\vec{r} \quad (10)$$

where we have simply retained the radial projection of the current vector \vec{j} . Some results for the Ar+Ti reaction are presented in figure 5 where the ratio $E_{coll}^{monop}/E_{coll}$ is plotted as a function of time respectively for $E/A=20$ MeV

(fig. 5.a) and $E/A=44$ MeV (fig. 5.b) laboratory energy. After the maximum compression stage at which E_{coll}^{monop} naturally almost vanishes, it is clear, in the case of $E/A=44$ MeV, that during the expansion phase E_{coll}^{monop} represents a dominant contribution to the total collective energy even when unbound

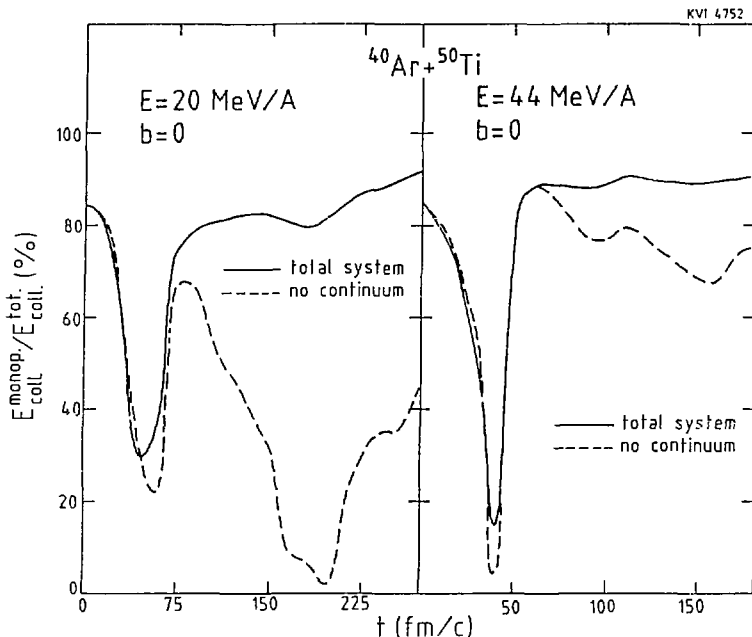


FIGURE 5

Time evolution of the ratio between monopole-like kinetic collective energy E_{coll}^{monop} (Eq. (10)) and the total collective energy E_{coll} (Eq. (4)) for the Ar+Ti reactions at two bombarding energies ($E/A=20$ MeV, figure (5.a), and $E/A=44$ MeV, figure (5.b)). The dashed line represents the result obtained without unbound particles.

particles ("continuum") are not taken into account. At lower energy the situation is less clear, which presumably reflects the increasing role of the large amplitude monopole motion only with increasing laboratory energy. It should however be noted that E_{coll}^{monop} should not be simply associated to a monopole mode, but rather gives an indication on the nature of the dominating process.

Provided one hence assumes that most of the collective energy is of monopole nature in the transition region (typically 80% for $E/A = 30$ MeV) one way to describe the instability is to consider the hydrodynamical frequency associated to the system. By writing the collective energy as

$$E_{coll} = \frac{1}{2} B \dot{\langle r^2 \rangle} \quad (11)$$

(within inserting the inertia parameter B and writing the time derivative as $\dot{\quad}$), and expressing the intrinsic energy as

$$E_{int} = \frac{1}{2} k \langle r^2 \rangle \quad (12)$$

where k defines the stress constant, one can simply estimate the hydrodynamical frequency $\lambda\Omega$ as

$$(\lambda\Omega)^2 = \frac{k}{B} \quad (13)$$

The system is hence in the unstable region when $(\lambda\Omega)^2 < 0$ and it is consequently easy to estimate the transit time inside the spinodal line.

In figure 6 $(\lambda\Omega)^2$ is plotted as a function of time for the Ar+Ti reaction at various laboratory energies. While at very low energy ($E/A=5$ MeV) $(\lambda\Omega)^2$ always remains positive one sees that even at 20 MeV/A some negative values are obtained but only over a very small time period. Anyhow one has to keep in mind the assumption of pure monopole mode (Eqs. 11-12) which for that case may be somewhat questionable. A striking point, clearly independent of this question is the fact that at 35 MeV/A the system stays in the spinodal region for a very long time and indeed explodes! At even higher energy (44 MeV/A) the expanding system has so much kinetic energy that it is able to cross the entire region of instability and finally does not stay that long in it. The interesting point is hence the clear transition at around 30 MeV/A lab energy between a regime in which the system, even if it flirts with the instability, does not stay long enough in this region to explode, and a regime in which it stays typically more than 120-150 fm/c and consequently explodes. This transition can be very clearly seen in figure 7 where we have plotted the transit time in the spinodal region versus the bombarding energy for the Ar+Ti reaction. Although the accuracy of the values plotted may be discussed within some percents because of the monopole analysis of the system, the order of magnitude transition around 30 MeV/A bombarding energy is however far beyond possible uncertainties!

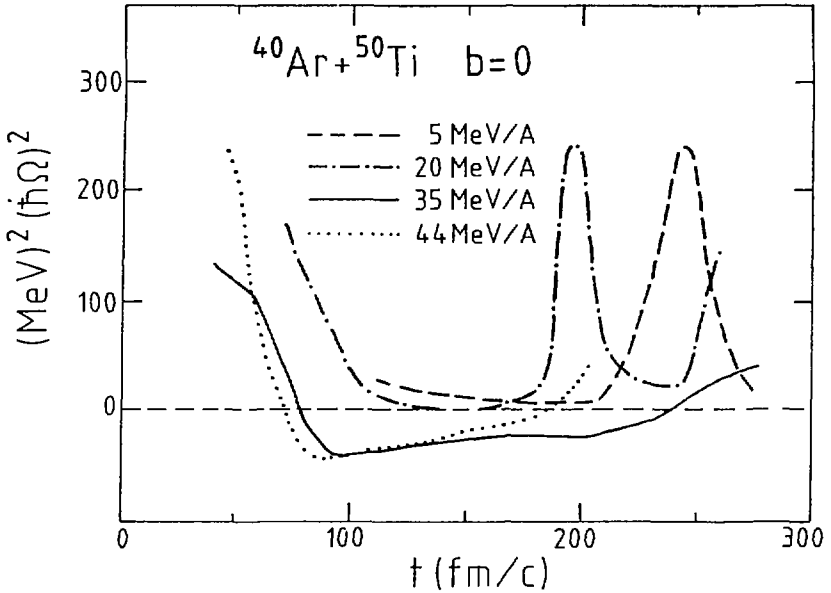


FIGURE 6

Time evolution of the square of the hydrodynamical frequency $(\hbar\Omega)^2$ (Eq. (13), in $(\text{MeV})^2$) for the Ar+Ti central reactions at various bombarding energies. The passage in the spinodal region corresponds to negative values of $(\hbar\Omega)^2$.

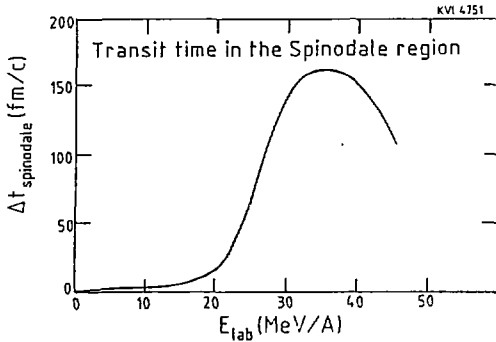


FIGURE 7

Transit time in the spinodal region (cf. also figure 6) versus the bombarding energy (E/A in MeV) for central Ar+Ti reactions. Note the order of magnitude transition around $E/A=30$ MeV.

Before concluding this analysis let us discuss the influence on our results of the nuclear matter compressibility K_∞ . The calculations presented above have been obtained with a Skyrme interaction of "standard" compressibility

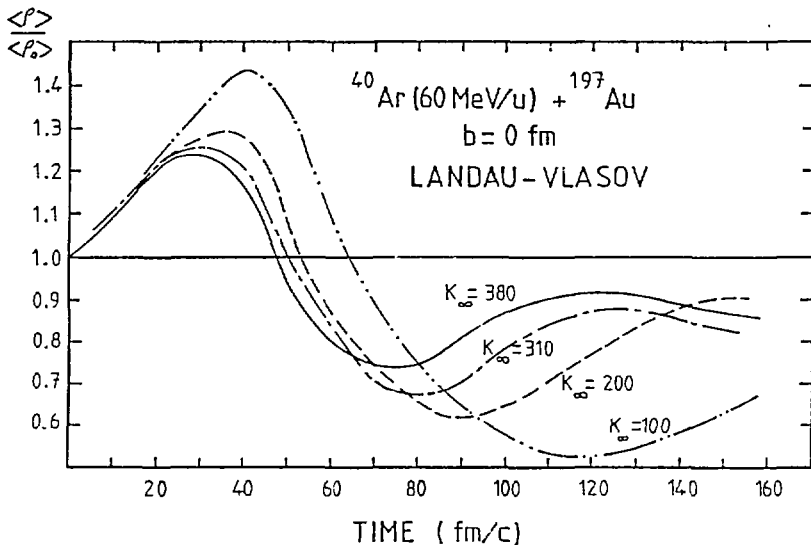


FIGURE 8

Variation of the ratio $\langle \rho \rangle / \langle \rho_0 \rangle$ between the average density and the equilibrium density as a function of time for the $^{40}\text{Ar} + ^{197}\text{Au}$ system at 60 MeV/A and for various compressibility moduli K_∞ ranging from 100 MeV to 380 MeV.

$K_\infty = 200$ MeV. As the kind of reactions we have studied allows to explore an intermediate range of the EOS, namely densities between 0.5 and 2 times the saturation density, it seems particularly interesting to study the influence of K_∞ on the disappearance of fusion. Figure 8 indicates that the deviation from the normal density scales as $1/\sqrt{K_\infty}$, as far as the amplitude is concerned. Keeping in mind that the spinodal region corresponds to densities smaller than 2/3 of the saturation density, it is clear that the softer the EOS, the deeper is the penetration into the spinodal region. In other words, for heavy asymmetric systems like Ar + Au, one should expect a multifragmentation cross section increasing with decreasing compressibility modulus. In the example of Figure 8, multifragmentation would occur at this

bombarding energy only for $K_{\infty} < 150$ MeV. The situation is probably different for light symmetric systems and requires further investigations. In these cases, the spinodal line can be reached easily even for moderate energies like 30 MeV/A, whatever K_{∞} is (assumed smaller than 400 MeV). The onset of multifragmentation would be governed by the transit time inside the spinodal region. As a matter of fact we have also made calculations with an interaction corresponding to a stiff EOS ($K_{\infty} = 350$ MeV), for the Ca+Ca system. In that case it seems that fusion actually disappears at a somewhat lower bombarding energy than in the $K_{\infty} = 200$ calculations. The system undergoes a compression phase up to a maximum compression which strongly depends on the lab energy, contrarily to the case of the soft EOS (see figure 3), but essentially possesses the same collective energy as the "soft" one. It is interesting to try to figure out how these results can be connected to actual properties of the EOS and of the expanding system. Following our analysis, and in the spirit of Ref. [10], the crucial quantity (Eq. (3)) is given by the product of the growth rate Γ times the transit time in the spinodale region Δt_{trans} . From the example of figure 8 one can assume that Δt_{trans} roughly scales as $1/\sqrt{K_{\infty}}$. The growth rate is directly connected to the sound velocity c_s in the medium. Two "asymptotic" cases can be easily worked out. The first one corresponds to a system without 2-body collisions (a Fermi liquid) and Γ is then proportional to c_s^2 and hence to K_{∞} , so that in that case $\Gamma \Delta t_{\text{trans}}$ (which gives a rough estimate of the integral Eq. (3)) should scale as $\sqrt{K_{\infty}}$. On the contrary, in the ultra collisional case (hydrodynamical limit) Γ is proportional to c_s or $\sqrt{K_{\infty}}$ so that $\Gamma \Delta t$ should be more or less independent of the compressibility. Our numerical results seem to lie somewhat in between these 2 situations (which once more confirms the relevance of microscopic realistic studies!) which presumably emphasizes the complexity of the mixing between mean-field and 2-body correlation effects. A more systematic study is hence necessary, in order to allow for a more complete interpretation of the results and for a better understanding of the interplay between mean-field and 2-body correlations.

6. CONCLUSION

In this note we have presented a microscopic study of the quasi-fusion/explosion transition in intermediate energy heavy-ion reactions ($E/A \sim 10-100$ MeV/A), within using a simulation of the Landau-Vlasov equation. We have shown the usefulness of such dynamical approaches as compared to qualitative schematic models. By extracting the kinetic collective energy we have obtained

an "Equation of State" of the Ca+Ca reaction at various incident energies. The explosion of the composite systems may then be connected, in this equation of state, to the crossing of the isentropic spinodal line. More precisely, by estimating the transit time Δt_{trans} during which the system actually stays in the mechanically unstable region ($K \leq 0$) we have been able to map out the explosion threshold to a sudden change in Δt_{trans} , from some fm/c to more than 100 fm/c, at around 30-35 MeV/A lab energy. This result qualitatively agrees with recent schematic estimates [10]. Finally we have presented a preliminary investigation of the dependence of the explosion threshold on the nuclear matter compressibility K_∞ . A more detailed interpretation of these results is in progress but already constitutes a promising task as it allows for exploring an intermediate region ($0.5 \rho_0 < \rho < 2\rho_0$) of the Equation of State.

ACKNOWLEDGEMENTS

One of the authors E.S. thanks the KVI for its warm hospitality and is glad to acknowledge the numerous enlightening discussions he had with R. Malfliet and O. Scholten. Two of us D.B. and M.P. also thank the ISN where they have done part of this work. L.Csernai, C.J. Pethick, F. Saint-Laurent, H. Schulz and H. Wolter are also thanked for fruitful discussions.

REFERENCES

- 1) A.D. Panagiotou, M.V. Curtin, H. Toki, D.K. Scott and P.J. Siemens, Phys. Rev. Lett 52 (1984) 496.
- 2) R. Balescu, Equilibrium and non equilibrium statistical mechanics, John Wiley ed., New York (1975).
- 3) G.F. Bertsch and P.J. Siemens, Phys. Lett. 126B (1983) 9.
- 4) J. Cugnon, Phys. Lett. 135B (1984) 374.
- 5) Ch. Grégoire, B. Remaud, F. Sébille, L. Vinet and Y. Raffray, Nucl. Phys. A465 (1987) 317.
- 6) J. Aichelin and H. Stöcker, Phys. Lett. 163B (1985) 59.
- 7) D.H.E. Gross, L. Satpathy, Ta. Chung Meng and M. Satpathy, Zeit. Phys. A309 (1982) 41.
- 8) J.P. Bondorf, R. Donangelo, I.N. Mishutin, C.J. Pethick, H. Schulz and K. Sneppen, Nucl. Phys. A443 (1985) 321.
- 9) J. Desbois, Nucl. Phys. A466 (1984) 724.

- 10) C.J. Pethick and D.G. Ravenhall, Nucl. Phys. A471 (1987) 19c and H. Heiselberg, C.J. Pethick and P.G. Ravenhall, Preprint Illinois University at Urbana-Champaign, 88/5/61 (1988).
- 11) E.A. Uehling and G.E. Uhlenbeck, Phys. Rev. 43 (1933) 552
- 12) G.F. Bertsch and S. das Gupta, Phys. Rep. 160C (1988) 189.
- 13) M. Raviart, Cours CEA, unpublished.
- 14) G. Welke, E. Suraud, Ch. Grégoire, R. Malfliet and M. Prakash, in preparation.
- 15) M. Krook and T.T. Wu, Phys. Rev. Lett. 36 (1976) 1107.
- 16) J.P. Blaizot, Phys. Rep. 64C (1980) 171.